Observation of Z-Dependent Impurity Accumulation in the PBX Tokamak

K. Ida,[a] R. J. Fonck, S. Sesnic, R. A. Hulse, and B. LeBlanc
Plasma Physics Laboratory, Princeton University, Princeton, New Jersey 08544
(Received 23 January 1986)

Charge-dependent convective impurity transport is observed in the central core of PBX H-mode discharges by measurement of radial profiles for both low- and high-Z intrinsic impurities in the presence of strong sawtooth activity. The time-evolving $Z_{\rm eff}$ profile and central metallic densities are modeled to yield a diffusion coefficient and a Z-dependent inward convective pinch which are in general agreement with estimates of neoclassical transport in the central plasma region.

PACS numbers: 52.25.Vy, 52.55.Fa

Impurity behavior in tokamak plasma experiments is observed to vary markedly from experiment to experiment, with conflicting results obtained even for nominally similar conditions.[1] Given competing neoclassical, rotation-driven, and anomalous transport mechanisms, it is important to characterize each situation experimentally as completely as possible. This is complicated, however, by the difficulty of obtaining data of sufficient quantity and quality to allow quantitative measurement of all relevant densities, gradients, and fluxes. Despite these problems, progress has been made and experimental results demonstrate a strikingly wide range of behavior, from plasmas where large anomalous diffusive fluxes ($D\sim10^4$ cm^2/sec) dominate, to others showing strong central impurity accumulation where neoclassical fluxes are often seen as sufficient to explain the observations.

While studied both qualitatively and sometimes quantitatively[2] in the past, the topic of central impurity accumulation and its possible causes continues to attract interest as a limiting mechanism for plasmas in the H-mode confinement regime with auxiliary heating,[3] near the density limit,[4] and of course in plasmas which are subject to strong toroidal rotation.[5-7] Most of these observations are concerned with discharges near or at a thermal collapse or disruption limit, and the plasma is necessarily heavily contaminated in such extreme conditions. It thus becomes necessary to study the behavior of all ion species present in order to consider possible transport mechanisms acting in the accumulated plasmas.

We present here an advance in detailed observations of impurity behavior in just such an accumulating case for neutral-beam-heated plasmas in the Princeton beta experiment (PBX) tokamak,[8] and concentrate on providing measurements of the simultaneous behavior of all ion species present which may influence the dynamics. The impurity transport coefficients themselves are derived via a novel modeling approach which uses the time-varying impurity distributions produced by naturally occurring sawtooth oscillations.

The discharges discussed here had plasma major radius of 148 cm, toroidal magnetic field of 1 T, plasma current of 300–330 kA, safety factor of ~5, line-averaged electron density of $(5.4\text{–}6.2)\times10^{13}$ cm^{-3}, injected beam power of 2.4–3.2 MW (co-perpendicular and co-tangential D^0 injection), and $T_i(0)\approx2.1$ keV. The plasma cross-sectional shape is noncircular, being shaped like a kidney bean with a midplane half-width of $a=36$ cm. The vertical elongation was $\kappa\simeq1.4$ and the plasma was bounded by a free separatrix, giving rise to a local expanded boundary divertor region and allowing operation with H-mode plasmas. To provide simultaneous observation of almost all relevant plasma parameters, a wide variety of diagnostics was employed, including visible continuum detectors, bolometers, soft-x-ray pulse-height analyzers, Thomson scattering, and vacuum UV and charge-exchange–recombination spectroscopy.

Impurity accumulation in the PBX tokamak is observed in Ohmic discharges with no sawtooth and in relatively dirty beam-heated discharges (both L and H mode) with either H^+ or D^+ background plasma. This accumulation is most easily studied in H-mode discharges because of improved particle confinement and relatively long sawtooth periods ($t_{\rm st}\gtrsim40$ ms) which are comparable to particle transport time scales.

At moderate beam powers ($P_{\rm inj}=2.4$ MW), the central $Z_{\rm eff}$ profile for an H-mode plasma is peaked and shows a periodic modulation whose drops coincide with the sawtooth seen with soft-x-ray diodes. The average impurity density is redistributed to be roughly flat immediately after the internal disruption, but then recovers to a peaked distribution as a result of strong inward convection before the next sawtooth drop. With an increase in beam power to 3.2 MW, the sawtooth period becomes very long ($\gtrsim100$ msec).[9] Detailed radial profiles of plasma parameters and impurity distributions are shown in Fig. 1 at a time near the end of this period where the plasma profiles and impurity influx are only slowly varying. It is clear from Fig. 1(b) that the high-Z impurities have a much more peaked profile than the low-Z impurities (i.e., O^{8+}), but the dominant metallic impurities, Ni [$n_{\rm Ni}(0)/n_e(0)=0.002$] and Fe (0.001), only contribute a value of $\lesssim1$ to $Z_{\rm eff}(0)$. The remaining $Z_{\rm eff}$ is due to the low-Z impurities ($n_{\rm C}\sim n_{\rm O}$) and hence the $Z_{\rm eff}$ profile in Fig. 1(c) resembles the O^{8+} profile in Fig. 1(b). The central radiated-power profile is determined mainly by the peaked metallic impurities, and the level of radiation

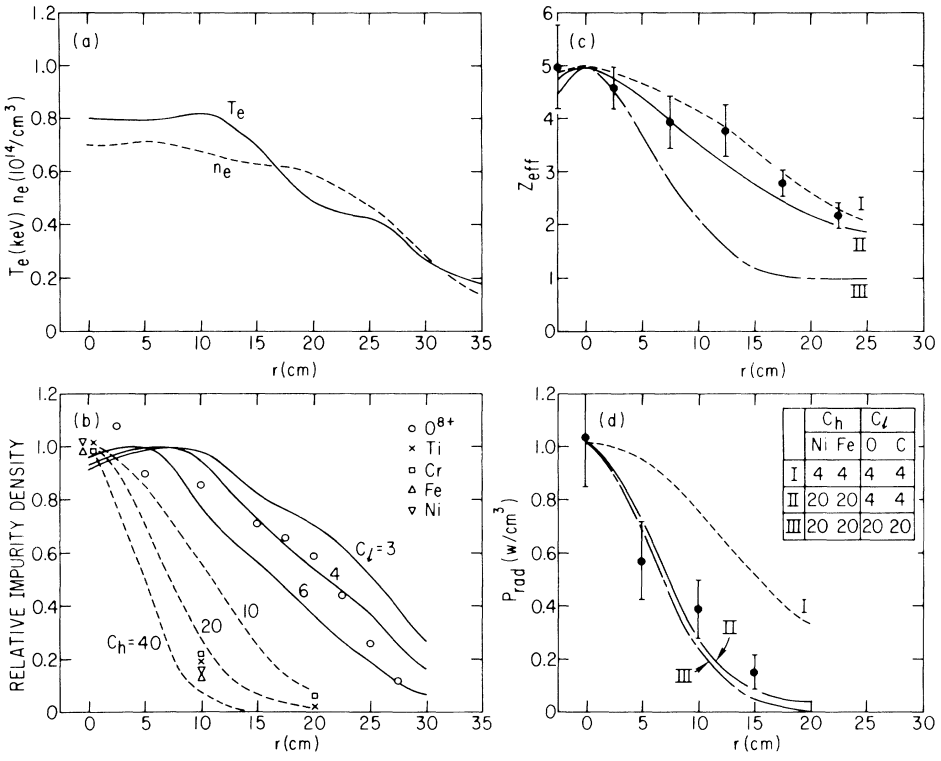

	C_h		C_l	
	Ni	Fe	O	C
I	4	4	4	4
II	20	20	4	4
III	20	20	20	20

FIG. 1. Impurity and plasma-parameter profiles for a long-sawtooth case: (a) plasma electron density and temperature profiles from Thomson scattering; (b) relative density profiles of O^{8+} (via charge-exchange–recombination spectroscopy) and several metallic species (via x-ray pulse-height analysis) along with calculated profiles for various impurity peaking parameters c_l and c_h; radial profiles of (c) Z_{eff} from visible bremsstrahlung measurements and (d) radiated power from bolometers.

is enough to cause the flattening of the electron temperature profile for $r \lesssim 10$ cm.

The solid and dashed curves shown with the data in Figs. 1(b)–1(d) represent corresponding solutions of the coupled radial continuity equations for all charge states of a given impurity-ion species, as calculated from the impurity transport code MIST,[10] which includes all relevant atomic processes in addition to radial transport. For these simulations, cylindrical symmetry is assumed and the radial flux for a given ion species of charge $+q$, Γ_q, is modeled by a simple diffusive-convective model with differing coefficients for low- and high-Z impurities:

$$\Gamma_q = -D_i \partial n_q/\partial r - c_i(2rD_i/a^2)n_q, \quad (1)$$

where n_q is the density of charge state $+q$, a is the plasma minor radius, and $v_i = -c_i 2rD_i/a^2$ is the radial convective velocity where the subscript $i = l$ or h stands for low- or high-Z impurities, respectively. The diffusion coefficients, D_i, and the convective-term peaking factors, c_i, are taken to be independent of radius for the core region.

The calculated profiles corresponding to the several measured parameters are shown in Fig. 1 for several values of c_i. While the results in Fig. 1(b) are obtained by our considering individual impurity species, the calculated $Z_{eff}(r)$ and radiated power profiles in Figs. 1(c) and 1(d) are obtained by including all major impurities using the measured absolute densities of metallic ions and the measured O^{8+} to C^{6+} ratio while normalizing to the central value of $Z_{eff}(0)$. The Z_{eff} and radiated power profiles for three pairs of c_l,c_h values are shown with the data in Figs. 1(c) and 1(d). Only the $c_l = 4$, $c_h = 20$ case is consistent with both of these measurements, as well as with the specific ion measurements in Fig. 1(b).

Since the above steady-state profile analysis gives only the ratio of the convective to diffusive fluxes, as represented by the peaking factor c_i, the time-evolving data with sawteeth are used to derive absolute transport coefficients for the core region. For example, Fig. 2(a) shows a detailed time evolution of $Z_{eff}(0)$ from visible bremsstrahlung measurements and use of model plasma profiles, along with the central metallic densities from pulse-height-analyzer measurements. The Z_{eff} data with vertical error bars represent points obtained with the measured $n_e(r)$,$T_e(r)$ profiles from Thomson scattering. The corresponding Z_{eff} profiles are seen in Fig. 2(b).

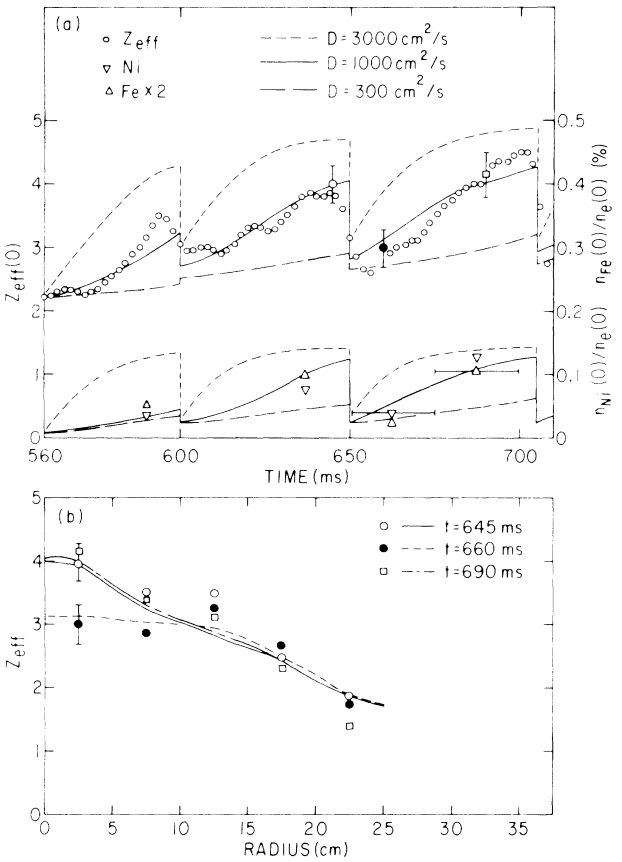

FIG. 2. (a) Time evolution of $Z_{\text{eff}}(0,t)$ and central metallic densities in the presence of strong sawteeth, compared with results of the transport code for various values of the diffusion coefficient. (b) Measured and calculated Z_{eff} profiles at three times with respect to the sawtooth phase. The corresponding central values are indicated in (a). For both cases, $c_l = 4$, $c_h = 20$, and $r_{\text{mix}} = 20$ cm are used.

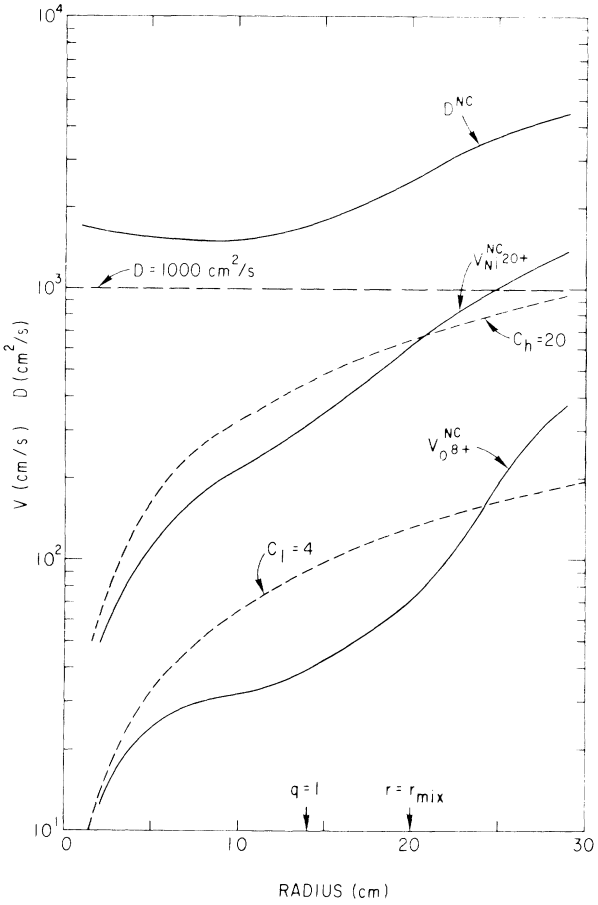

FIG. 3. Comparison of measured and estimated neoclassical transport coefficients as functions of radius. The solid lines are the neoclassical estimates, while reasonable fits to the data correspond to $D = 1000$ cm^2/s with $c_l = 4$ and $c_h = 20$, and are indicated by the dashed lines.

The solid and dashed curves in Fig. 2 are time-dependent solutions from the transport code which includes a redistribution of all impurities to a flat profile within a mixing radius given by $r_{\text{mix}} = 1.4 r_{\text{inv}}$ (where r_{inv} is the $q = 1$ inversion radius) at each internal disruption.[11,12] The peaking parameters $c_l = 4$ and $c_h = 20$ are taken from the long-sawtooth case discussed above, and the impurity edge influxes are adjusted to match the average increases of $Z_{\text{eff}}(0,t)$, $n_{\text{Ni}}(0,t)$, and $n_{\text{Fe}}(0,t)$ to the measurements. Given these values for c_i, the sawtooth-induced central variations provide a fairly precise discrimination for deriving values of D, the core impurity diffusion coefficient. Of course, the actual post-sawtooth repeaking is dominated by convection after the profiles flatten, but this convective transport is only implicitly determined by the chosen values of c_i and D in our model.

These transport coefficients are considerably different from those of experiments where no accumulation is observed, where $D \approx 10^4$ cm^2/sec and $c_v \approx 1$ are typical results.[1] Given that the observed transport characteristics are qualitatively similar to those expected by neoclassical theory, it is of interest to compare these results to such theory. A full time-evolving solution to the coupled continuity equations using completely accurate neoclassical fluxes, including all relevant species, is beyond the scope of this Letter, but we do show in Fig. 3 the model transport coefficients derived here (dashed lines) and steady-state transport coefficients obtained from collisional neoclassical fluxes[13] (solid lines) using the measured plasma and impurity profiles. (The difference in the neoclassical diffusion coefficients for low- and high-Z species is negligible for this case.) Contributions from all impurity species plus the plasma ions are included, with the dominant contributions arising from impurity-impurity–driven fluxes. While agreement between the model transport coefficients and the estimated neoclassical values is reasonably good in this plasma core region,

we emphasize that both the simplicity of our neoclassical model and the roughly factor of 2 uncertainties in the vlaues of c_i and D indicate that it is premature to conclude that detailed agreement with neoclassical theory has been obtained here. Rather, additional work is needed in both experiment and application of neoclassical theory to such experiments. In any event, the present results explicitly show a Z-dependent convective flux coupled with a relatively weak diffusive contribution in the central plasma region.

It is interesting to note that the degree of accumulation does not appear to correlate with the plasma rotation speed over the observed range of $v_\phi(0) = (0.1-2.0) \times 10^7$ cm/sec, and estimates of rotation-driven fluxes for these discharges indicate that they are considerably less than the impurity-impurity–driven inward flux for these co-injection plasmas.[14]

The present observations of impurity accumulation in either L- or H-mode discharges in the PBX tokamak with strong toroidal rotation in the co-plasma current direction are in contrast to other cases of accumulation for which improved H-mode confinement and strong counterinjection have been invoked as causative factors. While rotation-driven fluxes or changes in particle transport such as those attributed to H-mode conditions may indeed lead directly to central impurity accumulation, accumulation in contaminated plasmas with low central anomalous diffusion may also arise from the influence of secondary effects. For example, an increased impurity influx may in and of itself lead to a nonlinear dynamic process wherein the higher impurity concentrations lead to ever stronger central accumulation as impurity-impurity collisional effects dominate the transport. This suggests that strong accumulation may be avoided operationally by reduction of impurity influxes and lowering of the overall impurity levels, as has been observed.[14] These results, concurrent work on the Alcator-C experiment,[15] earlier work on smaller experiments,[2,16] and the possibility of large impurity-impurity–driven transport all emphasize the need for a full characterization of all ion constituents in the study of transport in any impure plasma, and especially when attempting to identify causes of strong central impurity accumulation.

The authors wish to thank E. Powell, G. Schmidt, M. Shimada, and G. Jahns for help and useful conversations. We also thank K. Bol, M. Okabayashi, and the PBX group for support and encouragement in this effort. This work was supported by the U.S. Department of Energy Contract No. DE-AC02-76-CHO-3073.

---

[a]Permanent address: Department of Physics, Faculty of Science, University of Tokyo, Bunko-ku, Tokyo 113, Japan.

[1]R. C. Isler, Nucl. Fusion **24**, 1599 (1984), and references therein.

[2]For example, K. H. Burrell *et al.*, Nucl. Fusion **8**, 1009 (1981).

[3]M. Keilhacker *et al.*, in *Proceedings of Tenth International Conference on Plasma Physics and Controlled Nuclear Fusion Research, London, 1984* (International Atomic Energy Agency, Vienna, 1985), Vol. I, p. 71.

[4]R. C. Isler, W. L. Rowan, and W. L. Hodge, Phys. Rev. Lett. **55**, 2413 (1985).

[5]S. Suckewer *et al.*, Nucl. Fusion **24**, 815 (1984).

[6]R. C. Isler, P. D. Morgan, and N. J. Peacock, Nucl. Fusion **25**, 386 (1985).

[7]W. M. Stacey *et al.*, Nucl. Fusion **25**, 463 (1985).

[8]M. Okabayashi *et al.*, in *Proceedings of Tenth International Conference on Plasma Physics and Controlled Nuclear Fusion Research, London, 1984* (International Atomic Energy Agency, Vienna, 1985), Vol. I, p. 229.

[9]K. Bol *et al.*, Phys. Rev. Lett. **57**, 1891 (1986).

[10]R. A. Hulse, Nucl. Technol. Fusion **3**, 259 (1983).

[11]F. H. Seguin, R. Petrasso, and E. S. Marmar, Phys. Rev. Lett. **51**, 455 (1983).

[12]K. Ida, R. J. Fonck, R. A. Hulse, and B. LeBlanc, Princeton Plasma Physics Laboratory Report No. PPPL-2264, 1985 [Plasma Phys. Controlled Fusion (to be published)].

[13]P. H. Rutherford, S. P. Hirshman, R. Jensen, D. E. Post, and F. G. P. Seidl, Princeton Plasma Physics Laboratory Report No. PPPL-1297, 1976 (unpublished).

[14]K. Ida, Ph.D. thesis, University of Tokyo, 1986 (to be published).

[15]R. Petrasso *et al.*, Phys. Rev. Lett. **57**, 707 (1986).

[16]S. A. Cohen, J. L. Cecchi, and E. S. Marmar, Phys. Rev. Lett. **35**, 1507 (1975).